Continuous control of the nonlinearity phase for harmonic generations

LI, Guixin; Chen, Shumei; Pholchai, Nitipat; Reineke, Bernhard; Wong, Polis Wing Han; Pun, Edwin Yue Bun; CHEAH, Kok Wai; Zentgraf, Thomas; Zhang, Shuang

Published in:
Nature Materials

DOI:
10.1038/nmat4267

Published: 26/06/2015

Continuous control of nonlinearity phase for harmonic generations

Guixin Li[1,2†], Shumei Chen[1,2†], Nitipat Pholchai[3,4,5], Bernhard Reineke[3], Polis Wing Han Wong[6], Edwin Yue Bun Pun[6], Kok Wai Cheah[2]*, Thomas Zentgraf[3]*, and Shuang Zhang[1]*

[1]School of Physics & Astronomy, University of Birmingham, Birmingham, B15 2TT, UK

[2]Department of Physics, Hong Kong Baptist University, Kowloon Tong, Hong Kong

[3]Department of Physics, University of Paderborn, Warburger Straße 100, D-33098 Paderborn, Germany

[4]Department of Industrial Physics and Medical Instrumentation, King Mongkut's University of Technology North Bangkok, 1518 Pibulsongkram Road, Bangkok 10800, Thailand

[5]Lasers and Optics Research Group, King Mongkut's University of Technology North Bangkok, 1518 Pibulsongkram Road, Bangkok 10800, Thailand

[6]Department of Electronic Engineering, City University of Hong Kong, 83 Tat Chee Ave, Hong Kong

*email: kwcheah@hkbu.edu.hk; thomas.zentgraf@uni-paderborn.de; s.zhang@bham.ac.uk;

The capability of locally engineering the nonlinear optical properties of media is crucial in nonlinear optics. Although poling is the most widely employed technique for achieving locally controlled nonlinearity, it leads only to a binary nonlinear state, which is equivalent to a discrete phase change of π in in the nonlinear polarizability. Here, inspired by the concept of spin rotation coupling, we experimentally demonstrate nonlinear metasurfaces with homogeneous linear optical properties but spatially varying effective nonlinear polarizability with continuously controllable phase. The continuous phase control over the local nonlinearity is demonstrated for second and third harmonic generation by using nonlinear metasurfaces consisting of nanoantennas of C3 and C4 rotational symmetries, respectively. The continuous phase engineering of the effective nonlinear polarizability enables complete control over the propagation of harmonic generation signals. Therefore, this method seamlessly combines the generation and manipulation of harmonic waves, paving the way for highly compact nonlinear nanophotonic devices.

The local phase of the nonlinear polarizability determines how the generated nonlinear light in the material will interfere during its generation and propagation processes. In general one is interested in a constructive conversion of the fundamental to nonlinear light while a wave is propagating through the material. However, chromatic dispersion prevents an efficient conversion owing to the different propagation velocities of light for different wavelengths. If the phase of the induced nonlinear material polarization can be controlled locally without modifying the linear properties, such a mismatch can be avoided and the nonlinear process would be more efficient. So far there has been no demonstration of a material that allows continuous and arbitrary phase control for the local nonlinear polarizability. Such a nonlinear material would enable exact phase matching conditions for nonlinear optical processes, in contrast to the widely used quasi-phase matching scheme, in which only the sign of the nonlinear polarizability can be manipulated[1-6]. It may remove further undesired nonlinear processes which are introduced by the higher Fourier components of the nonlinear susceptibility in a periodically poled system. Metamaterials, on the other hand, provide a high degree of freedom for tailoring the local optical properties on a subwavelength scale. Nevertheless, they have been mostly used for tailoring the linear optical properties.

The phase control over the nonlinear polarizability of the metamaterial is inspired by the concept of spin-rotation coupling of light, which has been used to control the light wavefront in the linear regime[7-11]. This novel concept has been applied to the design of various types of functional metasurface[12-16]. These types of metasurface, which consist of plasmonic structures with subwavelength feature sizes (sometimes called `artificial atoms'), can be engineered to show rotation-controlled local geometric phase shifts. This concept has been employed for flat lens imaging, generation of vortex beams, three-dimensional holography and optical spin-orbit interactions[12-17]. Here we apply the concept of spin-rotation coupling of light to the nonlinear regime, to realize to a nonlinear material polarization with an arbitrarily controllable phase profile. As a demonstration we show that this concept can be implemented by metasurfaces containing plasmonic antennas. However, the concept of continuous phase control is universal and can be applied also to dielectric and bulk-like metamaterials.

We start by considering a subwavelength plasmonic or dielectric nanostructure (resembling a dielectric dipole) embedded in an isotropic nonlinear medium (Fig. 1a). We will show that, when excited by a circularly polarized fundamental beam, the phase of the nonlinear polarization of the artificial atom can be controlled geometrically by the orientation of the structure through a spin-rotation coupling. For an incident fundamental beam with circular polarization state σ propagating along +z direction, the electric field can be expressed as: $\vec{E}^{\sigma} = \tilde{E}_0(\vec{e}_x + i\sigma\vec{e}_y)/\sqrt{2}$, where $\sigma = \pm 1$ represents the state of left- or right- handed circular polarization, respectively. The excitation of the nanostructures (for example, plasmonic nanorods) together with the nonlinear medium in the close vicinity of the structure, where the field can be strongly enhanced, locally forms an effective nonlinear dipole moment:

$$\vec{p}_{\theta}^{n\omega} = \vec{\alpha}_{\theta}(\vec{E}^{\sigma})^n \qquad (1)$$

where ω denotes the angular frequency of the fundamental beam, and α_{θ} is the n^{th} harmonic nonlinear polarizability tensor of the nanostructure with orientation angle of θ. We employ a coordinate rotation to analyse the dependence of the nonlinear dipole moment on the orientation angle of the nanostructure. In the local coordinates of the nanostructure (referred to as the local frame), as shown in Fig. 1a, where the local coordinate (*x'*, *y'*) axes are

rotated by an angle of θ with respect to the laboratory frame (x, y), the fundamental wave acquires a geometric phase owning to the spin-rotation coupling effect

$$\vec{E}_L^{\sigma} = \vec{E}^{\sigma} \mathrm{e}^{i\sigma\theta} \tag{2}$$

where the index 'L' denotes the nanostructure's local coordinate frame. The n^{th} harmonic nonlinear polarizability in the structure's local frame is simply $\alpha_{0\theta}\big|_{\theta\alpha=}{}_{=0}$. Thus, the n^{th} harmonic nonlinear dipole moment in the local frame is given by

$$\vec{p}_{\theta,L}^{n\omega} = \ddot{\alpha}_0 (\vec{E}_L^{\sigma})^n = \ddot{\alpha}_0 (\vec{E}^{\sigma})^n e^{in\sigma\theta} \tag{3}$$

The nonlinear dipole moment can be decomposed into two in-plane rotating dipoles (characterized by the circular polarization states σ and -σ) as

$$\vec{p}_{\theta,L}^{n\omega} = \vec{p}_{\theta,L,\sigma}^{n\omega} + \vec{p}_{\theta,L,-\sigma}^{n\omega} \text{ with } \vec{p}_{\theta,L,\sigma}^{n\omega}, \vec{p}_{\theta,L,-\sigma}^{n\omega} \propto e^{in\sigma\theta} \tag{4}$$

After transforming back to the laboratory frame the two rotating dipole moments are given by

$$\begin{aligned} \vec{p}_{\theta,\sigma}^{n\omega} &= \vec{p}_{\theta,L,\sigma}^{n\omega} e^{-i\sigma\theta} \propto e^{(n-1)i\sigma\theta} \\ \vec{p}_{\theta,-\sigma}^{n\omega} &= \vec{p}_{\theta,L,-\sigma}^{n\omega} e^{i\sigma\theta} \propto e^{(n+1)i\sigma\theta} \end{aligned} \tag{5}$$

The nonlinear polarizabilities of the nanostructure can therefore be expressed as,

$$\begin{aligned} \alpha_{\theta,\sigma,\sigma}^{n\omega} &\propto e^{(n-1)i\sigma\theta} \\ \alpha_{\theta,-\sigma,\sigma}^{n\omega} &\propto e^{(n+1)i\sigma\theta} \end{aligned} \tag{6}$$

Thus, geometric phases of $(n-1)\sigma\theta$ or $(n+1)\sigma\theta$ are introduced to the nonlinear polarizabilities of the n^{th} harmonic generation with the same or the opposite circular polarization to that of the fundamental wave, respectively. According to the selection rules for harmonic generation of circular polarized fundamental waves, a single nanostructure with m-fold rotational symmetry only allows harmonic orders of $n \quad lm\pm=1$, where l is an integer, and the '+' and '-' sign correspond to harmonic generation of the same and opposite circular polarization, respectively[18-21]. The phases of the nonlinear polarizability for an incident fundamental wave of circular polarization, for various orders of harmonic generation and nanostructures of various rotational symmetries, are given in the Supplementary Materials (Table **1**).

Hence, for a nanorod structure with two-fold rotational symmetry (C2), third harmonic generation (THG) signals with both the same and opposite circular polarizations to that of the fundamental wave can be generated. According to equations (3), (4), they have spin-dependent phases of $2\theta\sigma$ and $4\theta\sigma$, respectively (Fig. 1b). On the other hand, a nanostructure with four-fold rotational symmetry (C4) does not allow a THG process for the same polarization state as the incident polarization. Hence, only a single THG signal, that of the opposite circular polarization, is generated, with a geometric phase of $4\sigma\theta$ (Fig. 1c). Importantly, owing to the local isotropic response of the C4 structure, both the polarization state and the propagation of the fundamental wave will not be affected when transmitting through a metamaterial consisting of such C4 nanostructures of arbitrary orientation. Thus, by assembling the C4 nanostructures with spatially varying orientations in a three-dimensional (3D) or 2D lattice, a nonlinear metamaterial or metasurface can be formed that shows homogeneous linear properties, but locally a well-defined nonlinear polarizability distribution for a circularly polarized fundamental wave.

We verify this concept of spin-rotation-induced nonlinear phase by designing and fabricating three nonlinear binary phase gratings consisting of 2D arrays of plasmonic nanocrosses with a local C4 rotational symmetry (Fig. 2a-c). These binary nonlinear phase gratings can be easily used to characterize the relative phase of the nonlinear polarization between C4 nanostructures of different orientations. Sample A consists of nanocrosses of identical orientation along the entire lattice and a periodicity of a = 400 nm in both x- and y- axis directions, whereas Samples B and C consist of supercells of nanocrosses with two different orientations and a superperiod of P = 3.2 μm (eight crosses per unit cell). The difference between the orientation angles of the two subsets I and II of nanocrosses within a unit cell is π/8 and π/4 for *Sample B* and C, respectively. For the C4 structures, only THG of the opposite circular polarization to that of the incident fundamental beam is generated, with a geometric phase of 4 $\theta\sigma$. Thus, the introduced nonlinear phase for Samples B and C corresponds to nonlinear phase gratings with phase differences of π/2 and π between the two subunits, respectively, between the two subunits. For a binary nonlinear grating with period larger than the THGwavelength, the distribution of the nonlinear signal in different diffraction orders is determined solely by the phase difference between the two subsets. Thus, by experimentally measuring the ratio between the zeroth- and first-order THG signals, we are able to verify the orientation-induced phase difference between the two subsets of nanocrosses within a unit cell in Samples B and C.

First, we coat a nonlinear active medium (PFO) on top of these three phase gratings to form a gold/PFO hybrid metasurface (see Methods). The linear optical properties of the hybrid phase gratings are characterized by using Fourier transform infrared spectrometry. From the measured transmission spectra (Fig. 2d), we identify that the localized plasmon resonance is at a wavelength λ ~ 1230 nm for all three samples, as also confirmed by the numerical simulation. Subsequently, we measured the THG signal from these three samples for a fundamental wavelength at the resonance dip to maximize the plasmon-enhanced nonlinear response from the samples. As shown previously[22-30], the combination of the strong field enhancement and large nonlinear polarizability of the plasmonic structures gives rise to a large nonlinear optical effect in such a plasmonic system, making it easy to detect the generated nonlinear signal.

In the next step we illuminated the samples with short laser pulses at 1,240nm and measured the THG signal on a charge coupled device (CCD) camera. Our THG measurements with circular polarized incident light confirm the selection rules for the C4 symmetry structure as the THG signals with identical polarization states to the fundamental wave (RCP-RCP and LCP-LCP) are very weak for all three samples, and therefore not visible in Fig. 2e. Sample A, with a spatially homogeneous orientation of the nanocrosses, gives rise only to a zeroth-order THG. On the other hand, Samples B and C, with superlattice periodicities greater than the wavelength of the THG light, emit THG into the first diffraction order. For Sample B, where the phase difference between the third-order nonlinearity of the two subsets of nanocrosses is π/2 the ratio between the zeroth-order and first-order THG signals is predicted to be ~ 2.4:1 (see Supplementary Materials Fig. S1 and the corresponding discussion). The measured ratio is around 2.8:1, which agrees very well with the theoretical prediction. The π phase difference between the nonlinear polarizabilities of the two subsets of the nanocrosses in Sample C is expected to result in complete destructive interference for the zeroth-order THG signal, which is confirmed by the measurement shown in the rightmost panel of Fig. 2e. The orientation-angle-dependent phase of nonlinearity is further confirmed by numerically calculating the contribution to the far-field THG radiation from each

local point in the nonlinear medium, as shown in Supplementary Figs 2 and 3. The simulation results provide an intuitive picture how the phase of the contribution varies with the orientation angle of the nanostructure for circularly polarized incident light.

Having confirmed the possibility for geometric phase control of the nonlinear polarizabilities through variation of the orientation of the nanoantennas, we constructed and fabricated two metasurfaces consisting of an array of plasmonic nanostructures with C2 (nanorod) and C4 (nanocross) rotational symmetry. For these samples, the orientation angle between the neighbouring structures is varied linearly to obtain a linear phase gradient for the nonlinear polarization along the surface direction (Fig. 3a, b). Such a phase gradient will lead to a tailored diffraction for the THG signal, where the diffraction angle is determined by the phase gradient.

The linear diffraction of these metasurfaces for the fundamental beam is characterized at wavelengths of 1.2 μm and 1.25 μm for the C2 and C4 metasurfaces, respectively, corresponding to their respective resonance wavelengths. The diffraction pattern, captured by an infrared CCD camera, is shown in Fig. 3c. For the C2 metasurface, the local anisotropy leads in the linear optical case to conversion between LCP and RCP, with a geometric phase given by twice the orientation angle of the nanorods. Whereas the zeroth-order has the same circular polarization as the incident beam, the beam with the opposite circular polarization is diffracted into the +1 or -1 order, depending on the incident circular polarization state. This diffraction effect arises from the spin-dependent geometric phase in the linear regime, which has been investigated previously[12]. On the other hand, there is no diffraction observed for the C4 metasurface, as locally the nanocrosses exhibit isotropic linear optical properties. Therefore, the C4 metasurface can be considered as a homogeneous optical surface in the linear regime, despite the spatial variation of the orientation angle along the surface.

THG measurements on the C2 and *C*4metasurfaces for circularly polarized incident beams were subsequently carried out and the expected results for these two surfaces with the linear phase gradient are schematically illustrated in Fig. 4a.We observe that THG signals with the same and opposite polarization to that of the incident fundamental beam are generated on the C2 metasurface, whereas only the THG signal with the opposite circular polarization is generated on the C4 sample. This again agrees with the selection rules for THG in nanostructures with different local symmetries. For the C2 sample (Fig. 4b), the THG signal is generated in four different diffraction orders, -2, -1, +1 and +2, which correspond to the incident/transmitted polarization of RCP/LCP, RCP/RCP, LCP/LCP and LCP/RCP, respectively. This can be explained by equations (1), (2), where the nonlinear phases for the parallel polarization and opposite polarization are $2\sigma\theta$ and $4\ \sigma\theta$, respectively, corresponding to the ±1 and ±2 diffraction orders for the C2 metasurface with a period of the orientation angle:$\pi= \theta\Delta$. On the other hand, for the C4 metasurface, only THG with polarization opposite to that of the incident beam is generated with the phase gradient of $4\ \sigma\ \theta$, which corresponds to the first diffraction orders for the C4 metasurfaces with period of $\theta\Delta =\pi/2$ for the orientation angle. For a circularly polarized dipole in the x-y plane, the emitted THG into a diffraction angle of φ in general contains both LCP and RCP components, with the ratio given by $(1 -\cos(/)\ \varphi 1+ \cos\varphi)$. The periodicities of the nonlinear gratings in our work is 3.2μm and the THG wavelength is 416nm for the C2metasurfaces. The diffraction angle φ of the first diffraction order for the THG signal is calculated as 7.5 ° , agreeing well with our measurement. As the diffraction angle is small, the THG signal is almost a circularly polarized

beam, with the ellipticity given by $\psi = \tan^{-1}[(E_R - E_L)/(E_R + E_L)] = 0.991$. This is in agreement with our observation that the nonlinear signal is almost purely circularly polarized (Fig. 4b). The measurement nicely demonstrates the great potential for such spin-rotation-induced nonlinear phases in metamaterials: the C4 nonlinear nanostructures have orientation-independent linear properties whereas the phase of the nonlinear polarization is orientation-controlled by the building blocks of the material. Such properties are highly attractive for constructing nonlinear photonic devices such as nonlinear photonic crystals. It should be noted that the pump light needs to be at normal incidence, so that rotational symmetry of the overall system is maintained. For light at oblique incidence, it is expected that non-trivial effects due to superposition of multipole contributions will affect both the linear and nonlinear properties[31].

As mentioned earlier, this concept of controlling the nonlinear phase is not confined to THG, but can be applied to any harmonic order. As a confirmation of this claim we measured the second harmonic generation (SHG) for a metasurface consisting of C3 rotational symmetric structures for a linear phase gradient in the nonlinear polarization (Supplementary Fig. 4). These measurements correspond to the same situation as shown in Fig. 4, but for SHG instead of THG, and validate that the concept works also for other nonlinear processes.

Our work demonstrates that, through the spin-rotation coupling of light with subwavelength-sized nanostructures, a local continuous phase can be introduced into the nonlinear harmonic generation processes with metamaterials. We show that, through this scheme, we are able to continuously tune the phase of the nonlinear polarization in a metasurface consisting of nanocrosses with spatially varying orientations while preserving homogeneous linear optical properties. By controlling the local symmetry and global phase profile, spin-dependent third harmonic diffraction from the non-linear metasurface is experimentally demonstrated and agrees well with the theoretical predictions. Despite demonstrating a nonlinear metasurface with a phase gradient of the nonlinear polarizability along only one direction, our metasurface can be readily designed and realized to have more complex phase profiles in two in-plane directions, similar to the 2D nonlinear photonic crystals first proposed by V. Berger[32] and experimentally realized by Broderick and colleagues[33]. On the other hand, our metasurface goes beyond those previous works because of the continuous nonlinear phase profile, providing more powerful selection of the nonlinear reciprocal vectors involved in the nonlinear processes (for example, by removing the higher frequency components unavoidable with the discrete poling steps). One key application of 2D nonlinear metasurfaces is the realization of nonlinear holograms, where a beam at the fundamental wavelength can be converted to an arbitrary beam profile at a different wavelength. The continuous nonlinear phase profile of our metasurface would enable better control of the beam profile, meanwhile removing the issue of twin image generation that is intrinsic to a binary hologram. This approach for continuously controlling the nonlinearity can be potentially extended to 3D metamaterials made from low-loss nonlinear dielectric nanostructures, to achieve custom-defined local effective nonlinear susceptibilities, and introduce new degrees of freedom for designing nonlinear materials satisfying perfect phase matching conditions, nonlinear photonic crystals with arbitrary nonlinear phase profiles, and the manipulation of nonlinear signals in integrated photonic circuits or in free space.

Methods

Sample Fabrication. All the gold nanorods, of thickness 30 nm, were fabricated on glass substrates using standard electron beam lithography (Crestec CABL-9510C) followed by lift-off processes. All the gold metasurface devices were coated with a 100-nm-thick poly(9,9-dioctylfluorence; PFO) layer to form metal/organic hybrid nonlinear metasurfaces. Our previous studies have shown that the THG effciency in the PFO/gold hybrid metasurface is much higher than that from PFO- or gold-only devices[21], indicating that the high nonlinear response is a combination of the field enhancement from the plasmonic structures and the large nonlinear coeffcient of the PFO. In this work, enhanced THG from the hybrid metasurface enables easier detection of THG signals using a CCD camera.

THG Measurement. The diffraction of the harmonic generation was measured using a femtosecond (fs) laser (repetition frequency: 80MHz, pulse duration: ~ 200 fs) output from an optical parametric oscillator at a wavelength that is close to the localized plasmon resonance wavelengths of the nanostructures. The average power of the pumping laser is 30mW. The laser, with a spot diameter of ~ 80 μm, is incident normally on the metasurface after passing through an achromatic lens (f =100 mm). The THG signals from the gold/PFO metasurfaces are collected by an infinity-corrected objective lens (40x, NA = 0.6).The back-focal plane of the objective lens was imaged onto a CCD camera after filtering out the pump laser wavelength using bandpass filters.

References

1. Armstrong, J. A., Bloembergen, N., Ducuing, J. & Pershan, P. S. Interactions between light waves in a nonlinear dielectric. *Phys. Rev*. **127**, 1918-1939 (1962).
2. Fejer, M. M., Magel, G. A., Jundt, D. H. & Byer, R. L. Quasi-phase-matched second harmonic generation: tuning and tolerances. *IEEE J. Quantum Electron*. **28**, 2631-2654 (1992).
3. Zhang, X., Lytle, A. L., Popmintchev, T., Zhou, X., Kapteyn, H. C., Murnane, M. M. & Cohen, O. Quasi-phase-matching and quantum-path control of high-harmonic generation using counterpropagating light. *Nat. Phys.* **3**, 270-275 (2007).
4. Ellenbogen, T., Voloch-Bloch, N., Ganany-Padowicz, A. & Arie, A. Nonlinear generation and manipulation of Airy beams. *Nat. Photon.* **3**, 395-398(2009).
5. Xu, P. & Zhu, S. N. Quasi-phase-matching engineering of entangled photons. *AIP Advances* **2**, 041401(2012).
6. Zhu, S. N., Zhu, Y. Y., Qin, Y. Q., Wang, H. F., Ge, C. Z. & Ming, N. B. Harmonic generation in a Fibonacci optical superlattice of $LiTaO_3$. *Phys. Rev. Lett*. **78**, 2752-2755 (1997).
7. Berry, M. V. Quantal phase factors accompanying adiabatic changes. *Proc. R. Soc. London Ser. A* **392**, 45-57(1984).

8. Bhandari, R. Phase jumps in a QHQ phase shifter - some consequences. *Phy. Lett. A* **204**, 188-192 (1995).

9. Gori, F. Measuring stokes parameters by means of a polarization grating. *Opt. Lett.* **24**, 584-586 (1999).

10. Bomzon, Z., Kleiner, V. & Hasman, E. Pancharatnam-Berry phase in space-variant polarization state manipulations with subwavelength gratings. *Opt. Lett*. **26**, 1424-1426 (2001).

11. Gorodetski, Y., Niv, A., Kleiner, V. & Hasman, E. Observation of the spin-based plasmonic effect in nanoscale structures. *Phys. Rev. Lett*. **101**, 043903 (2008).

12. Yu, N., Genevet, P., Kats, M. A., Aieta, F., Tetienne, J. P., Capasso, F. & Gaburro, Z. Light propagation with phase discontinuities: generalized laws of reflection and refraction. *Science* **334**, 333-337 (2011).

13. Ni, X., Emani, N. K., Kildishev, A., Boltasseva, V. A. & Shalaev, V. M. Broadband light bending with plasmonic nanoantennas. *Science* **335**, 427 (2012).

14. Chen, X., Huang, L. L., Mühlenbernd, H., Li, G. X., Bai, B., Tan, Q., Jin, G., Qiu, C. W., Zhang, S. & Zentgraf, T. Dual-polarity plasmonic metalens for visible light. *Nat. Commun*. **3**:1198 (2012).

15. Huang, L. L., Chen, X., Mühlenbernd, H., Zhang, H., Chen, S., Bai, B., Tan, Q., Jin, G., Cheah, K. W., Qiu, C. W., Li, J., Zentgraf, T. & Zhang, S. Three-dimensional optical holography using a plasmonic metasurface. *Nat. Commun*. **4**:2808 (2013).

16. Li, G. X., Kang, M., Chen, S. M., Zhang, S., Pun, E. Y. B., Cheah, K. W. & Li, J. Spin-enabled plasmonic metasurfaces for manipulating orbital angular momentum of light. *Nano Lett*. **13**, 4148-4151(2013).

17. Yin, X. B., Ye, Z. L., Rho, J., Wang, Y. & Zhang, X. Photonic spin Hall effect at metasurfaces. *Science* **339**, 1405-1407 (2013).

18. Yin, X. B., Ye, Z. L., Rho, J., Wang, Y. & Zhang, X. Photonic Spin Hall Effect at metasurfaces. *Science* **339**, 1405-1407 (2013).Burns, W. K. & Bloembergen, N. Third-harmonic generation in absorbing media of cubic or isotropic symmetry. *Phys. Rev. B* **4**, 3437-3450 (1971).

19. Bhagavantam, S. & Chandrasekhar, P. Harmonic generation and selection rules in nonlinear optics. *Proc. Indian Acad. Sci. A* **76**, 13-20 (1972).

20. Konishi, K. et al. Polarization-controlled circular second-harmonic generation from metal hole arrays with threefold rotational symmetry. Phys. Rev. Lett. 112, 135502 (2014).

21. Chen, S. M., Li, G. X., Zeuner, F., Wong, W. H., Pun, E. Y. B., Cheah, Zentgraf, T., K. W. & Zhang, S. Symmetry selective third harmonic generation from plasmonic metacrystals. *Phys. Rev. Lett.* **113**, 033901 (2014).

22. Kauranen, M. & Zayats, A. V. Nonlinear plasmonics. *Nat. Photon.* **6**, 737-748 (2012).

23. Kujala, S., Canfield, B. K., Kauranen, M., Svirko, Y. & Turunen, J. Multipole interference in the second-harmonic optical radiation from gold nanoparticles. *Phys. Rev. Lett.* **98**, 167403 (2007).

24. Zhang, Y., Grady, N. K., Ayala-Orozco, C. & Halas, N. J. Three-dimensional nanostructures as highly efficient generators of second harmonic light. *Nano Lett.* **11**, 5519-5523 (2011).

25. Cai, W., Vasudev, A. P. & Brongersma, M. L. Electrically controlled nonlinear generation of light with plasmonics. *Science* **333**, 1720-1723 (2011).

26. Aouani, H., Cia, M. N., Rahman, M., Sidiropoulos, T. P. H., Hong, M., Oulton, R. F. & Maier, S. A. Multiresonant broadband optical antennas as efficient tunable nanosources of second harmonic light. *Nano Lett.* **12**, 4997-5002 (2012).

27. Utikal, T., Zentgraf, T., Paul, T., Rockstuhl, C., Lederer, F., Lippitz, M. & Giessen, H. Towards the origin of the nonlinear response in hybrid plasmonic systems. *Phys. Rev. Lett.* **106**, 133901 (2011).

28. Renger, J., Quidant, R., Van Hulst, N. & Novotny, L. Surface-enhanced nonlinear four-wave mixing. *Phys. Rev. Lett.* **104**, 046803 (2010).

29. Rose, A., Powell, D. A., Shadrivov, I. V., Smith, D. R. & Kivshar, Y. S. Circular dichroism of four-wave mixing in nonlinear metamaterials. *Phys. Rev. B* **88**, 195148 (2013).

30. Suchowski, H., O'Brien, K., Wong, Z. J., Salandrino, A., Yin, X. & Zhang, X. Phase mismatch-free nonlinear propagation in optical zero-index materials. *Science* **342**, 1223-1226 (2013).

31. Kruk, K. S., Decker, M., Staude, I., Schiecht, S., Greppmair, M., Neshev, D. N., & Kivshar, Y. S. Spin-polarized photon emission by resonant multipolar nanoantennas. *ACS Photonics*, **1**, 1218-1223 (2014).

32. Berger, V. Nonlinear photonic crystals. *Phys. Rev. Lett.* **81**, 4136-4139 (1998).

33. Broderick, N. G. R., Ross, G. W., Offerhaus, H. L., Richardson, D. J., Hanna, D. C. Hexagonally poled Lithium Niobate: a two-dimensional nonlinear photonic crystal. *Phys. Rev. Lett*. **84**, 4345-4348 (2000).

Acknowledgments

This work was partly supported by EPSRC (EP/J018473/1). T.Z. and S.Z. acknowledge financial support by the European Commission under the Marie Curie Career Integration Program. N.P., B.R. and T.Z. acknowledge the financial support by the DFG Research Center TRR142 `Tailored nonlinear photonics'. K.W.C. and E.Y.B.P. acknowledge the support by the Research Grant Council of Hong Kong under Projects HKUST2/CRF/11G and AoE/P-02/12. G.L. acknowledges support from the High Performance Cluster Computing Centre, Hong Kong Baptist University. S.Z. acknowledges financial support from the National Science Foundation of China (grant no. 61328503) and Leverhulme Trust (grant no. RPG-2012-674).

Author contributions

SZ and TZ conceived the idea and experiment. BR, PWHW and EYBP fabricated the samples. GL, SC, NP, KWC and TZ performed the measurements. SC performed the simulation. GL, SZ and TZ wrote the paper. All authors participated in discussion.

Additional information

Competing financial interests

The authors declare no competing financial interests.

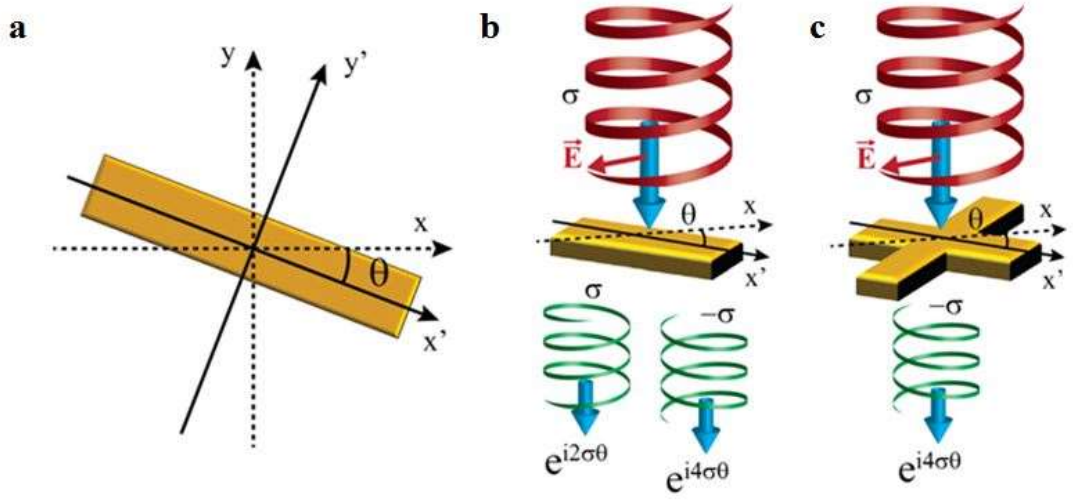

Figure 1| Illustration of geometric phase controlled nonlinear metamaterials. a, Rotating a nanostructure by an angle θ with respect to the laboratory frame will introduce a geometric phase. Hereby each nanostructure introduces a nonlinear geometric phase with a phase variation of (n-1)$\sigma\theta$ or (n+1)$\sigma\theta$ to the n^{th} harmonic generation for the same or the opposite circular polarization to that of the fundamental wave, respectively. **b**, For a *C*2 nanostructure, THG signals of both circular polarizations with phases of 2$\sigma\theta$ and *4*$\sigma\theta$ are generated in the forward direction. **c**, For a *C*4 nanostructure, only THG signals with a circular polarization opposite to that of fundamental wave is generated, which has a phase of *4*$\sigma\theta$.

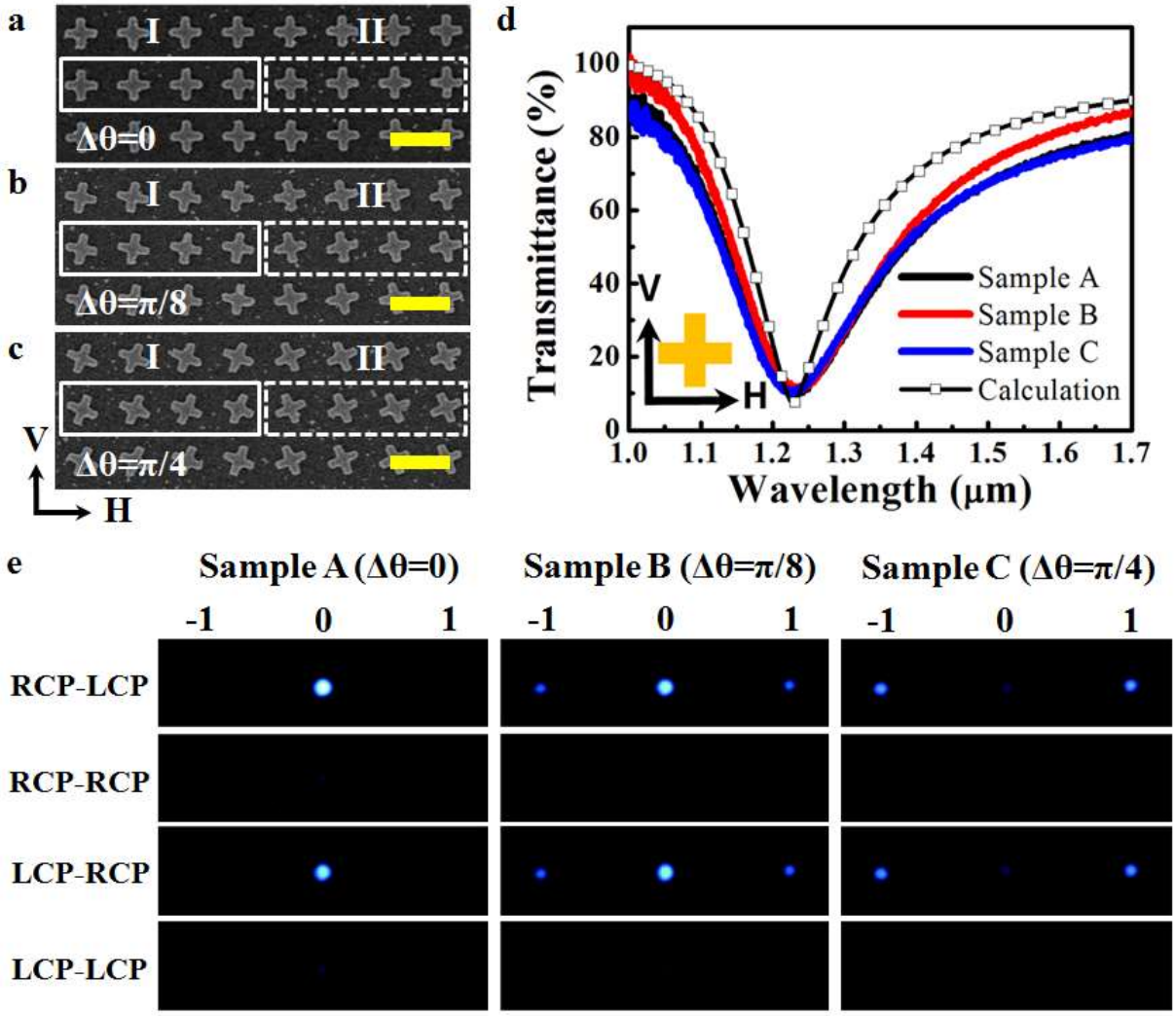

Figure 2| Experimental verification of the nonlinear phase with nonlinear phase gratings. **a-c**, Scanning electron microscopy images of Samples *A*, *B* and *C* fabricated by electron-beam lithography. Each unit cell can be divided into two subsets, I and II, that consist of nanocrosses with generally different orientations. The width and length of each gold nanorod are 50nm and 240 nm, respectively. The lattice sizes for the three metasurfaces are a= 400 nm along x- (H) and y- (V) axis directions; the thickness of gold layer is t = 30 nm. The scale bar shows 400 nm. **d**, Measured and simulated transmission spectra for the PFO coated hybrid metasurfaces showing the plasmonic resonance of the gold nanostructures for horizontal (H-) polarized illumination (see inset for the orientation of the axes). **e**, Measured diffraction pattern of THG signals from metasurfaces *A*, *B*, and *C*. The THG signals of the first and second rows correspond to right circularly polarized (RCP) pumping laser; the third and fourth rows corresponds to the left circularly polarized (LCP) pumping laser.

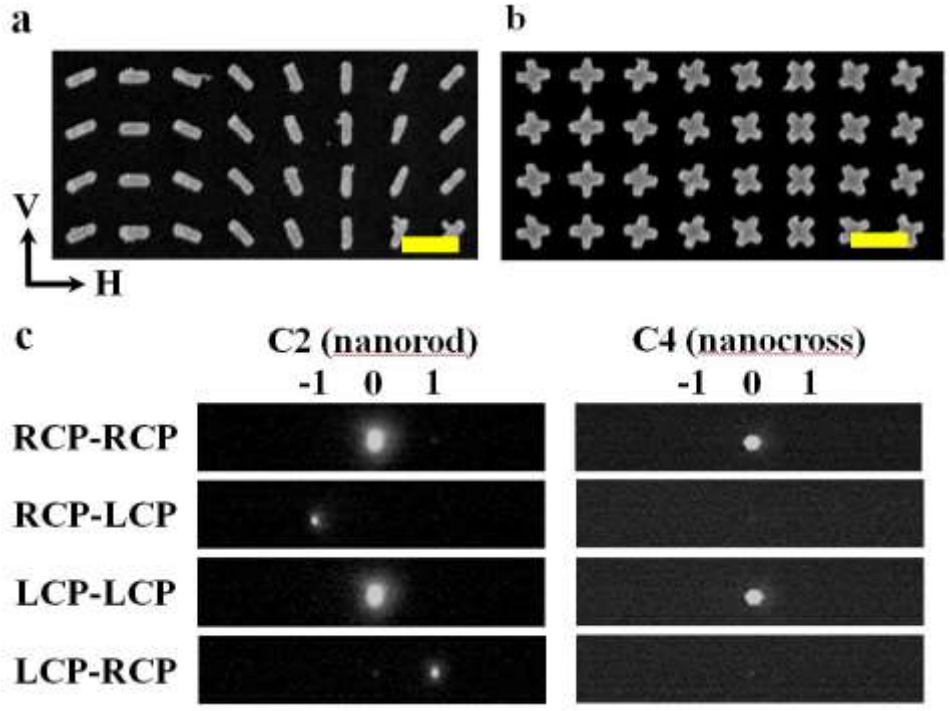

Figure 3| Diffraction of the fundamental wave on metasurfaces with linear phase gradients. **a**, **b**, Scanning electron microscopy images of metasurfaces consisting of *C*2 and *C*4 symmetry nanostructures. The lattice constant of the metasurfaces in both directions is a = 400 nm. Along the x direction (H) the nanostructures are rotated by an angle of $\pi/8$ for the *C*2 structures and $\pi/16$ for the *C*4 structures, resulting in the same superlattice period *P*=3.2 μm. scale bar: 400 nm. **c**, Measured diffraction pattern of the fundamental waves on the*C*2 (λ = 1250 nm) and the*C*4 (λ = 1200 nm) metasurfaces. The first and second rows were recorded using right circularly polarized (RCP) laser, while the third and fourth rows correspond to left circularly polarized (LCP) illumination.

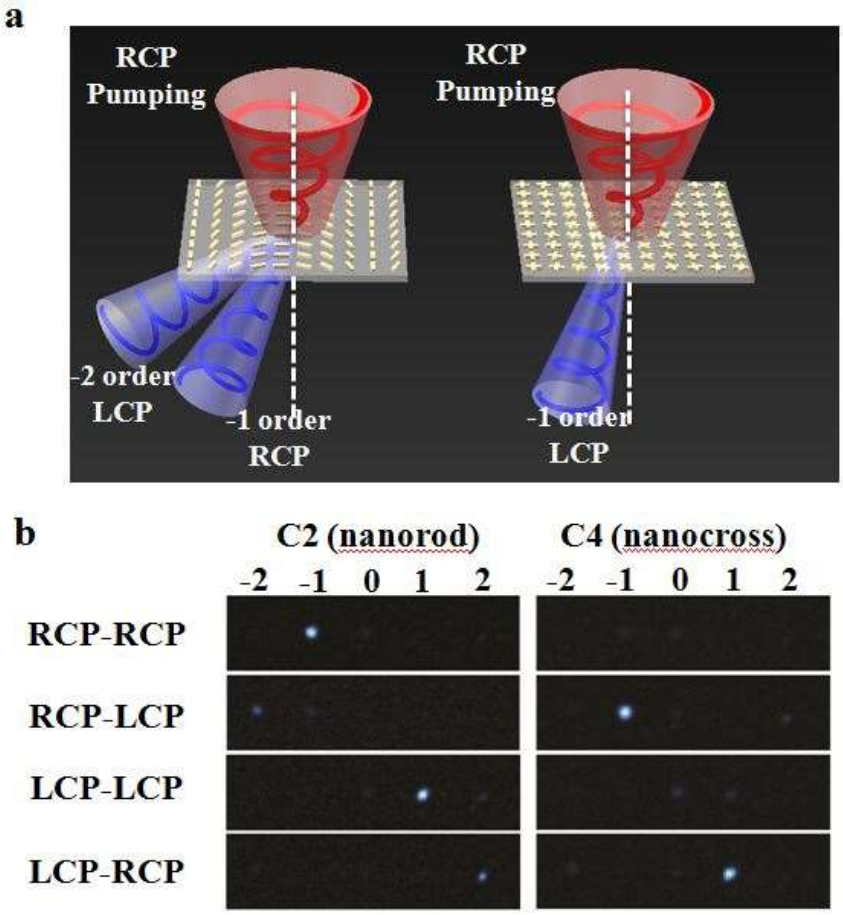

Figure 4| THG signals from metasurfaces with a phase gradient of the nonlinearity. a, Illustration of phase-controlled diffraction of THG signals for right circularly polarized (RCP) light at the fundamental frequency. The metasurfaces with *C*2 symmetry diffract right- (RCP) and left- (LCP) circularly polarized THG signals to the first and second orders, respectively; in comparison, the metasurface with *C*4 symmetry diffracts only the opposite circularly polarized THG signals in the first-order direction. **b**, Measured diffraction pattern of the THG signals from the *C*2/PFO and *C*4/PFO metasurfaces for circular polarization states of the fundamental and THG waves.